International Journal of Engineering Research
Volume No.9, Issue No.1, pp: 10-16
ISSN: 2319-6890 (online),2347-5013(print)
1 Jan. 2020

Study of a Cylindrical Crack Buried in an Infinite Mass under Indentation

Aly Rachid Korbeogo[(1)], Bernard K Bonzi[(2)], Gaël Pierson[(3)], Zacharie Koalaga[(1)], Richard N Kouitat[(3)]

[1]Joseph Ki-Zerbo University, Doctoral School of Science and Technology (EDST) Laboratory of Materials and Environment (LAME) Ouagadougou Burkina Faso
[2]Joseph Ki-Zerbo University Doctoral School of Science and Technology (EDST) Laboratory of Mathematics and Computer Science (LAMI) Ouagadougou, Burkina Faso
[3]University of Lorraine Jean Lamour Institute Department N2EV, UMR 7198 CNRS, Saurupt Park CS 14234, 54042 Nancy Cedex France Nancy, France

Corresponding Email: alykorbeogo@yahoo.fr

Abstract : We studied the cracking mechanisms encountered in some material. The phenomenon of pop in has caught our attention. To do this we have used the Boundary Element Method which in work has proven its effectiveness in dealing with three-dimensional cracking problems. The results obtained made it possible to simulate the hertz cones. Through this work we have simulated a crack that starts from the surface towards the inside. But the pop heard in indentation during cracking lets us think that the crack will open from the bottom up. Because in the other case, the noise would be absorbed.

Keys words: cylindrical crack, boundary element method, stress intensity factors

1. Introduction :

The study of cracking mechanisms under contact stress has already attracted the attention of many researchers. This work concerns almost all punch geometries. In the case of spherical punches, which induce the famous conical crack of Hertz, one can quote inter alia the work of Franck et al. [1], Mouginot et al. [2], Mouginot [3] and Bush [4]). Since then, the experimental devices for characterizing the mechanical behavior of surfaces have evolved with the advent of instrumented indentation systems coupled or not with an acoustic emission system. These devices allow the continuous acquisition of the evolution of the indentation depth as a function of the load (indentation curve). For some materials and in some cases, there is a discontinuity in the penetration depth for a given load. Among the many possible explanations for this phenomenon, there is the propagation of a buried or emergent crack. The work presented in this document aims to contribute to a better understanding of this phenomenon of "pop-in" by focusing on the case of cracks and a spherical punch. It should be noted that some work concerning spherical indentation cracking exists, but with particular attention to the creeping propagation of a surface defect. (e.g. Komovopoulos [5], Choi [6]). We present here a numerical study carried out with a tool based on the Boundary Element Method (BEM) which allows a short resolution time to treat three-dimensional crack problems very efficiently. (e.g., Cruse [7], Mi et al [8], Domiguez et al [9], Young [10], Bonnet [11], Aliabadi [12]). We first consider a cylindrical crack immersed in a solid, so the problem can be treated in three dimensions. Before loading, the initial fault is closed. After loading, it can remain, open partially or totally. It is therefore important to take into account the conditions of unilateral contact at the lips of the crack. To simplify the study, a perfect slip is admitted. We can note that the BEM is also a method of resolution well adapted for the problems of contact (eg Man and al [13], Dandekar and Conant [14], Takahashi and Brebbia [15], Olukoko and Becker [16], Karami [17]).

2. Problem definition

2.1. Statement of the problem

Consider a solid occupying a domain Ω of the frontier spaceΓ_n. We use the Cartesian coordinate system Ox_i with i = 1, 2, 3. We note Γc the surface of the crack. Volume forces are neglected, and Einstein's index notation and summation convention are adopted. The balance of forces and moments in the absence of volume forces is written in the given coordinate system:

$$\sigma_{ij,j} = 0 \quad dans \quad \Omega \backslash \Gamma_n \cup \Gamma_c \qquad (1)$$

With σthe Cauchy stress tensor, which in the case of linear elasticity in small deformations is related to the linearization tensor linearized by Hooke's law:

$$\sigma_{ij} = C_{ijkl}\varepsilon_{kl} \qquad (2)$$

In relation (2), $C_{ijkl}$is the fourth order isotropic tensor of the elastic constants of the material. It is expressed as a function of the shear modulus (G) and the Poisson's ratio (ν) by:

ISSN: 2319-6890 (online),2347-5013(print)
1 Jan. 2020

$$C_{ijkl} = G\left[\frac{2\nu}{1-2\nu}\delta_{ij}\delta_{kl} + \delta_{ik}\delta_{jl} + \delta_{il}\delta_{jk}\right] \quad (3)$$

$\delta_{ij}$is the Kronecker symbol such that:$\delta_{ij} = \begin{cases} 1 & si \quad i = j \\ 0 & \text{otherwise} \end{cases}$

The tensor of the small deformations $\varepsilon_{kl}$is defined starting from the vector displacement u by:

$$\varepsilon_{kl} = \frac{1}{2}\left(u_{k,l} + u_{l,k}\right) \quad (4)$$

Let's assemble equations (2) and (4) and equation (1) can be rewritten as:

$$C_{ijkl}u_{k,jl} = 0$$

The flow-type boundary conditions associated with this equation are of the form:
The flow-type boundary conditions associated with this equation are of the form:

$$t_i = \sigma_{ij}n_j \quad (6)$$

With $\vec{n}$the normal vector outside the considered boundary.

2.2 Method of solution

We use the so-called dual border element method [18]. The boundary of the domain is composed of the outer faces (Γ_n) and the crack $\Gamma_c$which is itself made up of two faces $\Gamma_c^+$and Γ_c^- so that$\Gamma_c = \Gamma_c^+ \cup \Gamma_c^-$. We introduce the displacement jump $\Delta u_j(x) = \Delta u_j(x^+) - \Delta u_j(x^-)$ and the constrained vector jump$\Delta t_j(x) = \Delta t_j(x^+) + \Delta t_j(x^-)$; x^+ (or. x^-) being a point, of the face Γ_c^+ (or.Γ_c^-), of geometric coordinate x. We limit ourselves to cases of symmetrically charged cracks. In this case, the discontinuity relation of the constrained vector disappears from the equations.
For any point belonging to the outer boundary of the environment, we adopt the classical integral formulation in displacement, namely:

$$\int_{\Gamma_n} T_{ki}(x,y)[u_i(y) - u_i(x)]dS(y) + \int_{\Gamma_c^+} T_{ki}(x,y)\Delta u_i(y)dS(y) = \int_{\Gamma_n} U_{ki}(x,y)t_i(y)dS(y) \quad (7)$$

For the points located on the upper face of the crack, we adopt the constraint vector formulation:

$$t_k(x) = \int_{\Gamma_n} \bar{T}_{ki}(x,y)u_i(y)dS(y) + \int_{\Gamma_c^+} \bar{T}_{ki}(x,y)\Delta u_i(y)\,dS(y) - \int_{\Gamma_n} \bar{U}_{ki}(x,y)\,t_i(y)\,dS(y) \quad (8)$$

In this formulation, the unknowns of the problem are the displacement and constraint vectors on the outer boundary, and displacement jump and stress on the faces of the crack.
The expressions of the influence functions that appear in equations (7) and (8) can be found in many works (e.g. [19, 20]). As already mentioned, the unknowns on the crack surfaces are the displacement jump vector $(\Delta\vec{u})$ and the stress vector $\vec{t}(x^+)$.
The outer boundary and the face of the upper crack are subdivided into a finite number of elements. Nine compliant and / or semi-discontinuous elements are used for the elements of Γn.

The elements of the surface of the crack are discontinuous. For the elements of the crack front, the interpolation introduced in Kouitat et al. [21] was adopted.
The discretized form of the boundary equations (eq. (7) and (8)) then leads to systems of equations of the following form:

$$[A^n]\{x^n\} = \{F^n\} - [B^n]\{\Delta u\}$$
$$\{T^c\} + [A^c]\{\Delta u\} = [\bar{G}]\{t^n\} - [\bar{H}]\{u^n\} \quad (9)$$

Where $\{x^n\}$is the vector of unknown nodal quantities on the outer boundary (displacements and constrained vectors); $\{\Delta u\}$is the vector of jumps of nodal displacements; {u ^ n} is the vector of nodal displacements on the outer boundary; $\{t^n\}$is the vector of nodal stress vectors on the outer boundary; $\{T^c\}$is the vector of the nodal stress vectors on the surface of the crack.
For the envisaged loading, the considered crack can be subjected to a mode of complex solicitation. On the face of the crack, the jumps of displacements and the constrainedvectors are not known in advance. The crack may be completely closed, partially closed or completely open. Consequently, it is necessary to impose a unilateral contact condition on the faces of the crack. At a point x of the surface of the crack, we introduce the local coordinate system$(\vec{n}(x), \vec{\tau}(x), \vec{\rho}(x))$. The vector $\vec{n}(x)$ designates the normal external to the surface of the crack at the point x such that $\vec{\tau}(x)$ and $\vec{\rho}(x)$ are two mutually orthogonal vectors, and tangent to the plane of the crack. Normal displacement discontinuity and normal stress must satisfy:

$$\Delta u_j n_j = -\Delta U_n \leq 0,\ t_j n_j = -t_n \leq 0 \quad et \quad t_n \Delta u_n = 0 \quad (10)$$

If the crack opens, then$\Delta U_n \neq 0$ and$t_n = 0$; otherwise $\Delta U_n = 0$ and$t_n \neq 0$.
We assume that the contact on the faces of the crack is frictionless. This indicates that the tangential components $(t_\tau \ et \ t_\rho)$of the constrained vector are identically zero.
We have chosen to solve equations (8) and (9), combined with the one-sided contact condition, by an iterative scheme whose algorithm is summarized below:

ISSN: 2319-6890 (online),2347-5013(print)
1 Jan. 2020

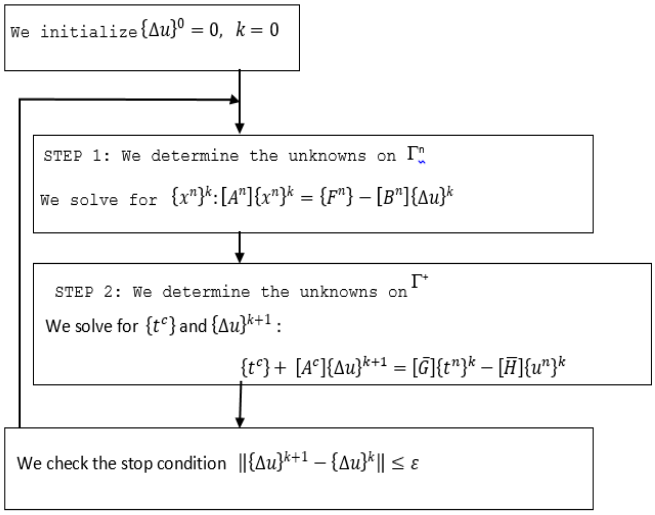

Where ε is the desired precision.

This algorithm can be seen as a different presentation of the superposition method to solve the crack problems presented by Ameen and Raghuprasad [22] and applied to 2D compression fracture problems by Elvin and Leung [23] and by De Bremaecker and al. [24]. In a previous work, compression cracking is formulated as a complementarity problem and solved by the "PATH solver" algorithm. The algorithm has been used successfully by Christensen et al in [25].

The matrix equation system solved in step 1 remains unchanged during the iterative process. The matrix of the system is then factorized once and for all and stored, which allows a computation time saving. In step 2, the system of equations must be completed by the contact equations. For each node of the crack boundary, we write:

$$\begin{cases} min(\Delta u_n, t_n) = 0 \\ t_\tau = 0 \\ t_\rho = 0 \end{cases} \quad (11)$$

The system obtained is therefore nonlinear and not differentiable in the classical sense. We applied Newton's method using Bouligand's differentiability (B-differentiability) presented in Christensen et al. [22] and Martin Schwartz [26]. We emphasize that the need for a directional derivative is due to the min function in equation (11).

The results presented in the following were obtained using this algorithm. In all the cases tested, the average number of iterations to converge with ε = 10-12 is about 15.

3. Results

To begin, consider a homogeneous solid, isotropic Young's modulus (E) equal to 220 GPa and Poisson's ratio (ν) equal to 0.3, of parallelepipedal shape. The base square of the parallelepiped of height 20 units of length has for side 10 units of length. It is oriented so that the height is in the z direction of the working reference (see Figure 1).

The boundary Γn is therefore composed of six faces of this geometry. Firstly, we consider that the lower face of the domain is simply supported, the upper face is subjected to a uniform load distribution and the lateral faces are free of tension.

The three factors called stress intensity factors determine the displacement of the crack lips by making a combination of three main modes denoted I, II and III.

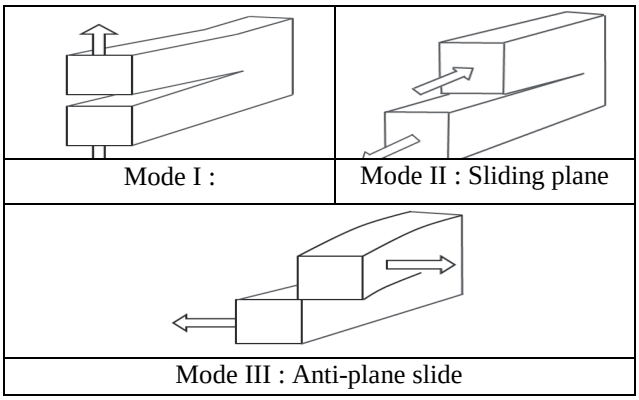

Fig. 1: Failure modes of a crack

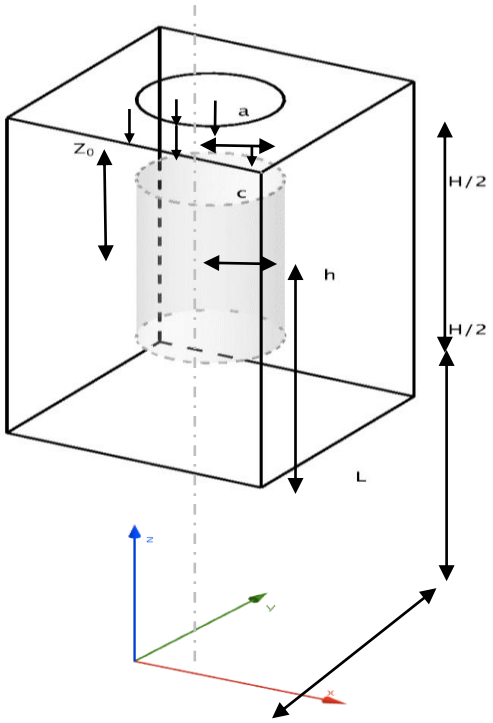

Fig.2: Geometry of the sample

c: radius of the crack, a: radius of the loading area

h: crack height, Z_0: position of the upper crack front with respect to the loaded surface. H: height of the room, L: length of a stop of the square base

In this parallelepiped we consider that there is an initial defect of crack type and cylindrical shape. We are interested in the

ISSN: 2319-6890 (online),2347-5013(print)
1 Jan. 2020

stability of this crack, according to its position in the medium and its dimensions compared to those of the basic geometry.For this study, we will use the stress intensity factors (KI, KII and KIII) and the energy release rate defined as:

$$G = \frac{1-\nu^2}{E}.(K_I^2 + K_{II}^2) + \frac{1+\nu}{E}.K_{III}^2 \qquad (12)$$

For our first calculations, the outer surface of the room is subdivided into 104 quadrilateral elements at nine nodes for a total of 502 nodes. The surface of the crack is made up of 80 nonconforming elements and 720 nodes. The results will be dimensioned using the factor K0 which corresponds to the stress intensity factor in mode I for a circular crack in tension in an infinite medium:

$$K_0 = 2\sigma\sqrt{\frac{c}{\pi}} \qquad (13)$$

σ denotes the charge density applied and c the radius of the crack.

3.1 Influence of the radius of the loading zone (a) at fixed c and h Consider first the case of a buried cylindrical crack of radius c = 2.5 and height h = 10 and centered in the parallelepiped. On different disks of radius a = 2; 2.5; 3; 3.5; 4; 4.5 and 4.75 of the upper face we apply a uniformly distributed load of density -1.10-3 MPa.
Numerical simulations lead to the following results:

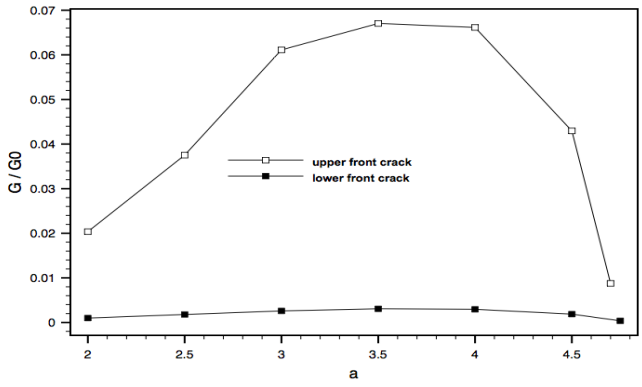

Fig.3: Propagation criterion according to the loading disk

The energy release rate G indicates that the larger the loading surface, the more the crack will remain closed. But we note that for a certain radius, here around 3, 5, the risk of crack propagation is highest.

This graph also allows us to say that if there is propagation it will be towards the top of the test piece (that is to say the loaded surface). So in some simulations we will only talk about the upper crack front.

Let us now consider the case of a truncated cone crack with a lower radius c = 2.5 and a radius greater than c = 1.25 with a height h = 10. The factors KI, KII, KIII and the restitution ratio G are shown in the figures below.

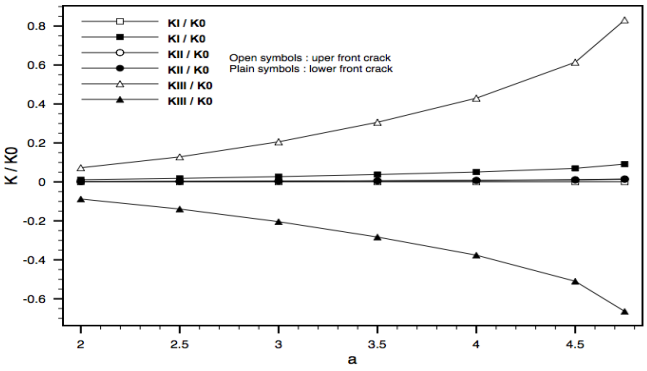

Fig.4: Stress intensity factors according to the loading disk

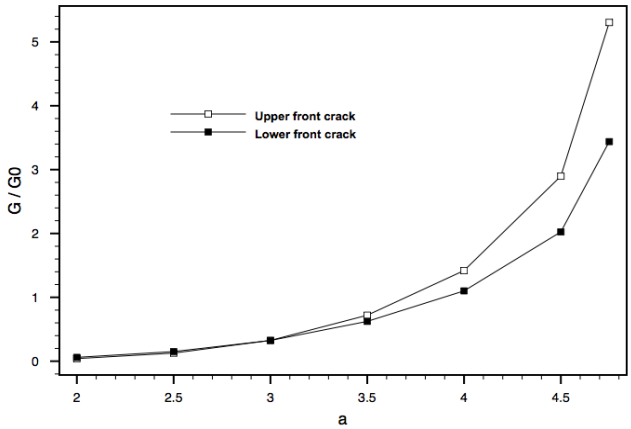

Fig.5: Propagation criterion according to the loading disk

In this case, KI and KII are almost zero on both fronts. For small loading radii, the KIII factors are almost equal in absolute value on both fronts. Their difference is appreciable only from a loading radius of 3.5 where that of the upper front becomes dominant. These results show us that if there is propagation, it will be in mode III and probably towards the loaded surface.For the cylindrical crack, we see that there is a maximum risk of propagation for a certain value. This maximum will be studied in the next part.

3.2 Influence of the position of the crack

The previous experiment allowed us to compare the propagation of the crack for a given position but it did not allow us to compare the propagation criterion G when the upper and lower crack fronts are located at the same depth z.
This is why we have resumed the experiment with a crack of height 2. We vary the factor Z0 between 0.5 and 7.5. It is useless to redo the experiment in the negative part of the cube because we see that the results of KI, KII, KIII and G all tend towards the same value. And we obtain the following graphs for stress intensity factors:

ISSN: 2319-6890 (online),2347-5013(print)
1 Jan. 2020

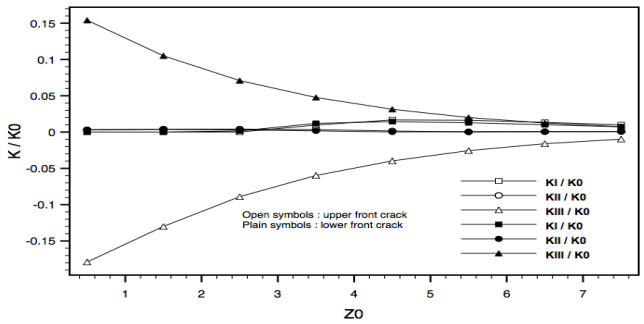

Fig.6: Stress intensity factors for both crack fronts atthe same time for a radius loading disk a = 2

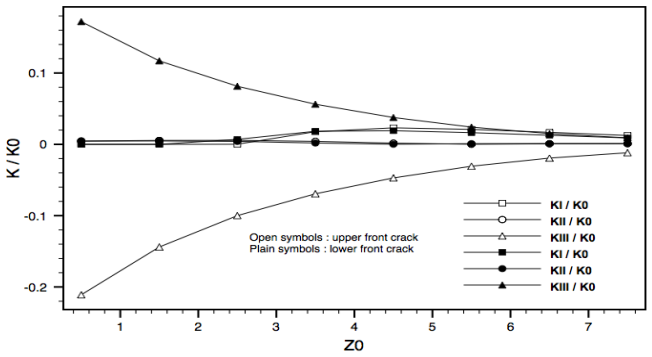

Fig.7: Stress intensity factors for both crack fronts at the same time for a radius loading disk a = 2.5

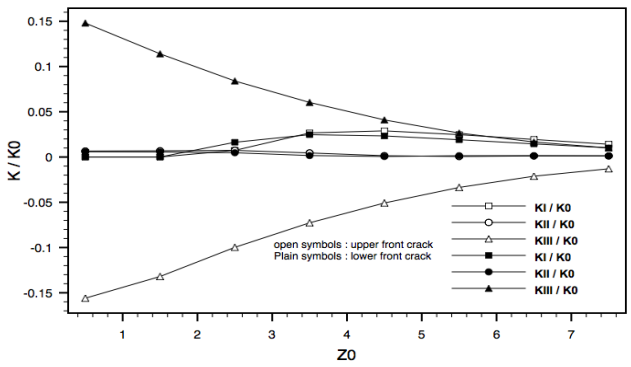

Fig.8: Stress intensity factors for both crack fronts at the same instant for a radius loading disk a = 3

At the level of the upper crack front, we note that the factor KII with respect to KIII is negligible. That is to say there would be a twist of the part inside the cylinder. Then for a crack size like this, we notice for both crack fronts that KI has the same profile. So our crack will be fully open for a Z0 between 3.5 and 7.5 units in length. The size of the crack influences the mode I aperture.

From the results, we can answer the problems that we asked ourselves before. If we look at comparing the KIII for the two lower (Z0 + h) and upper (Z0) crack fronts at the same z position (here on the graph, we compare the first point of the curve for the crack front lower than the third point for the upper crack front and we shift 1 each time for the others), we see that for the same ordinate z, the KIII factor of the lower crack front is larger than that of the upper crack front.

But for the same instant, it is larger on the upper crack front than lower.

In addition, the graph which represents the propagation criterion G as a function of the depth of the lower and upper crack front shows us that for the same z coordinate of the crack fronts, the lower crack will have a greater tendency to open than the upper crack. But at a given moment, the upper crack front has a higher propagation criterion than that of the lip of the lower crack. So our crack will also spread upwards.

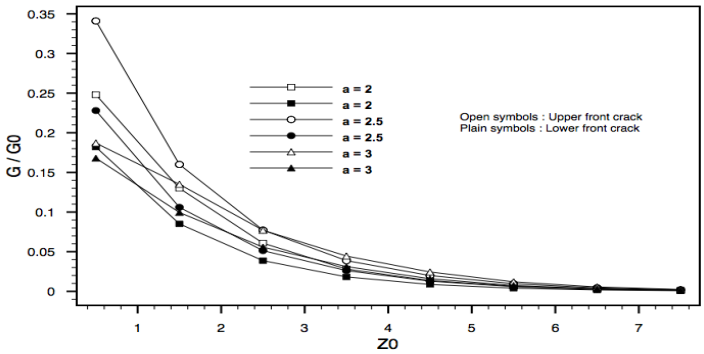

Fig.9: Propagation criterion G for both crack fronts at the same instant

To conclude on these two parts, if we compare the graphs which represent the propagation criteria G for a crack of height 10 and a crack of height 2, we notice a greater difference between the upper and lower crack fronts for a crack of large size only for a small crack.

When the crack is small, the propagation criteria for both fronts are almost equivalent and when it is large they are very different. The size of the crack has an influence on both crack fronts. The smaller the crack, the more edges will be linked.

4. Conclusion :

We see through this work that the BEM method is adapted to solve problems of fracture mechanics. This work has also shown that it was possible to open a circular crack front and see the evolution of a cylindrical crack. The open cylindrical cracks allowed us to see the appearance of a surface step and to compare it to an indentation experiment.

We have also shown that cracks can start from an impurity in the material as one might imagine in indentation. This work shows that the crack will evolve towards the surface if there is an internal defect.

These simulations also made it possible to simulate for the first time the hertz cones. Through this work we have simulated a crack that starts from the surface towards the inside. But the "pop" heard in indentation during cracking lets us think that the crack will open from the bottom up. Because in the other case, the noise would be absorbed.

ISSN: 2319-6890 (online),2347-5013(print)
1 Jan. 2020

Références

[i] Franck FC, Lawn RB. On the theory of Hertzian fracture. Proc Roy Soc A 1967; 299:291.

[ii] Mouginot R, Maugis D. Fracture indentation beneath flat and spherical punches. J Mater Sci 1985; 20:4354.

[iii] Mouginot R. Crack formation beneath sliding spherical punches. J Mater Sci 1987; 22:989.

[iv] Bush MB. Simulation of contact-induced fracture. Engng Anal Bound Elem 1999; 23:59.

[v] Komvopoulos K. Subsurface crack mechanisms under indentation loading. Wear 1996; 199:9.

[vi] Choi HJ. Effects of graded layering on the tip behavior of vertical crack in a substrate under frictional Hertzian contact. Engng Fract Mech 2001; 68:1033.

[vii] Cruse TA, Vanburen W. Three dimensional stress analysis of a fracture specimen with an edge crack. Int J Fract 1971; 71(1):1.

[viii] Mi Y, Aliabadi MH. Dual boundary element method for three-dimensional fracture mechanics analysis. Engng Anal Bound Elem 1992; 10:161.

[ix] Dominguez J, Ariza MP, Gallego R. Flux and traction boundary elements without hypersingular or strongly singular integrals. Int J Numer Meth Engng 2000; 48:111.

[x] Young A. A single-domain boundary element method for 3-D elastostatic crack analysis using continuous elements. Int J Numer Meth Engng 1996; 39:1265.

[xi] Bonnet M. Stability of crack fronts under Griffith criterion: a computational approach using integral equations and domain derivatives of potential energy. Comp Meth Appl Mech Engng 1999; 173:337.

[xii] Aliabadi MH. A new generation of boundary methods in fracture mechanics. Int J Fract 1997; 86:91.

[xiii] A. P. Cisilino, M. H. Aliabadi, Three-Dimensional Boundary Element Analysis of Fatigue Crack Growth in Linear and Nonlinear Fracture Problems, Engineering Fracture Mechanics, vol. 63, pp. 713–733, 1999.

[xiv] Man KW, Aliabadi MH, Rooke DP. Analysis of contact friction using the boundary element method. In: Aliabadi MH, Brebbia CA, editors. Computational methods in contact mechanics. Elsevier; 1993. R. Kouitat Njiwa, J. von Stebut / Engineering Fracture Mechanics 71 (2004) 2607–2620 2619

[xv] Dandekar BW, Conant RJ. Numerical analysis of contact problems using boundary integral equation method. Part I and II. Int J Numer Meth Engng 1992; 33:1513.

[xvi] Takahashi S, Brebbia CA. Elastic contact analysis with friction using the boundary elements flexibility approach. In: Aliabadi MH, Brebbia CA, editors. Computational methods in contact mechanics. Elsevier; 1993.

[xvii] Olukoko OA, Becker AA. A new boundary element approach for contact problems with friction. Int J Numer Meth Engng 1993; 36:2625.

[xviii] Karami G. Boundary element analysis of two-dimensional elastoplastic contact problems. Int J Numer Meth Engng 1993; 36:221.

[xix] A. P. Cisilino, M. H. Aliabadi, Three-Dimensional Boundary Element Analysis of Fatigue Crack Growth in Linear and Nonlinear Fracture Problems, Engineering Fracture Mechanics, vol. 63, pp. 713–733, 1999.

[xx] C. A. Brebbia, J. Dominguez, Boundary Elements: An Introductory Course, Computational Mechanics Publications, Billerica 1992.

xxi] M. Bonnet, Boundary Integral Equation Methods for Solids and Fluids, John Wiley and Sons, New York, 1999.

[xxii] R. Kouitat Njiwa, J. von Stebut, Three Dimensional Boundary Element Analysis of Internal Cracks under Sliding Contact Load with a Spherical Indenter, Engineering Fracture Mechanics, vol. 71, pp. 2607–2620, 2004.

[xxiii] M. Ameen, B. K. Raghuprasad, A Hybrid Technique of Modelling of Cracks Using Displacement Discontinuity and Direct Boundary Element Method, Int. J. Fract., vol. 67, pp. 343–355, 1994.

[xxiv] N. Elvin, C. Leung, A Fast Iterative Boundary Element Method for Solving Closed Crack Problems, Engng. Fract. Mech., vol. 63(5), pp. 631–648, 1999

[xxv] J. C. De Bremaecker, M. C. Ferris, D. Ralph, Compressional Fractures Considered as Contact Problems and Mixed Complementarity Problems, Engng. Fract. Mech., vol. 66, pp. 287–303, 2000.

[xxvi] P. W. Christensen, A. Klarbing, J. S. Pang, N. Strömberg, Formulation and comparison of algorithms for frictional contact problems, Int. J. Numer. Meth. Engng., vol. 42(1), pp. 145–175, 1998.

[xxvii] Martin Schwartz. Contribution to the resolution of three-dimensional problems of fragile cracking. Towards the use of a non-local model of elastic behavior. Other. University of Lorraine, 2018. French. NNT: 2018LORR0031. Tel-01749198